GPI- and Transmembrane-anchored Influenza Hemagglutinin Differ in Structure and Receptor Binding Activity

George W. Kemble,* Yoav I. Henis,‡ and Judith M. White*

*Department of Pharmacology and the Cell Biology Program, University of California, San Francisco, California 94143-0450; and ‡Department of Biochemistry, the George S. Wise Faculty of Life Sciences, Tel Aviv University, Tel Aviv, Israel 69978

Abstract. We investigated the influence of a glycosylphosphatidylinositol (GPI) anchor on the ectodomain of the influenza hemagglutinin (HA) by replacing the wild type (wt) transmembrane and cytoplasmic domains with a GPI lipid anchor. GPI-anchored HA (GPI-HA) was transported to the cell surface with equal efficiency and at the same rate as wt-HA. Like wt-HA, cell surface GPI-HA, and its ectodomain released with the enzyme PI-phospholipase C (PI-PLC), were 9S trimers. Compared to wt-HA, the GPI-HA ectodomain underwent additional terminal oligosaccharide modifications; some of these occurred near the receptor binding pocket and completely inhibited the ability of GPI-HA to bind erythrocytes. Growth of GPI-HA-expressing cells in the presence of the mannosidase I inhibitor deoxymannojirimycin (dMM) abrogated the differences in carbohydrate modification and restored the ability of GPI-HA to bind erythrocytes. The ectodomain of GPI-HA produced from cells grown in the presence or absence of dMM underwent characteristic low pH-induced conformational changes (it released its fusion peptides and became hydrophobic and proteinase sensitive) but at 0.2 and 0.4 pH units higher than wt-HA, respectively. These results demonstrate that although GPI-HA forms a stable trimer with characteristics of the wt, its structure is altered such that its receptor binding activity is abolished. Our results show that transmembrane and GPI-anchored forms of the same ectodomain can exhibit functionally important differences in structure at a great distance from the bilayer.

THE influenza virus hemagglutinin (HA)[1] is one of the best characterized membrane glycoproteins in terms of its structure, functions, biosynthesis, and membrane targeting. The structure of the HA trimer is known to high resolution (50). The glycoprotein functions as an adhesion molecule, a membrane fusion protein, and an immunogen (reviewed in 39, 47, 49). The primary translation product, HA0, folds and oligomerizes in the ER to form a homotrimer that is glycosylated and transported to the cell surface through the constitutive secretory pathway (2, 7, 22). In polarized cells, such as kidney epithelial cells and neurons, HA is targeted to specific membrane domains, the apical and axonal surfaces, respectively (15). Each mature HA monomer contains two disulfide-linked polypeptide chains, HA1 and HA2. The HA1 subunit contains the receptor binding site and major antigenic determinants; the HA2 subunit contains the fusion peptide, a sequence critical for membrane fusion (reviewed in 39, 47, 49).

HA is a type I integral membrane glycoprotein. Replacement of the HA transmembrane and cytoplasmic domains with those from other glycoproteins can alter HA assembly, transport, and subcellular localization (30, 35). Deletion of the HA transmembrane and cytoplasmic domains by the introduction of translation termination codons can result in the synthesis and secretion of improperly oligomerized polypeptides (7, 22, 37).

Unlike HA, many cellular proteins are embedded in membranes via a glycosylphosphatidylinositol (GPI) anchor (reviewed in 3, 10, 18). Several GPI-anchored proteins are involved in cell–cell adhesion, for example NCAM-1, T-cadherin, and sperm PH-20 (reviewed in 18, 41). Recently, an engineered GPI-anchored form of CD4 was shown to function as a receptor for the HIV envelope glycoprotein (25, 28). Therefore, both naturally occurring and engineered GPI-anchored proteins function as cell adhesion molecules. Some GPI-anchored molecules, such as LFA-3, NCAM-1

Dr. Kemble's present address is Aviron, 1450 Rollins Road, Burlingame, CA 94010.

Address correspondence to Judith M. White, Department of Pharmacology and the Cell Biology Program, University of California, San Francisco, CA 94143-0450.

1. *Abbreviations used in this paper*: DAF, decay accelerating factor; dMM, deoxymannojirimycin; GPI, glycosylphosphatidylinositol; HA, hemagglutinin; PK, proteinase K; wt, wild-type.

and the $F_c\gamma$ receptor, exist in both transmembrane and GPI-anchored forms (10), and these alternative forms can behave differently. GPI-anchored NCAM-1 is transported to the apical surface of polarized epithelial cells (4, 33); transmembrane-anchored NCAM-1 is transported to the basolateral surface (33). The route (36) and rate (26) of endocytosis of GPI- and transmembrane-anchored proteins differ. In addition to transport differences, GPI and transmembrane-anchored forms of the same polypeptide can have different activities. The lymphocyte surface molecules Ly-6/E and Qa-2 only activate T cells when present as GPI-anchored forms. The role of the GPI anchor in this process is, however, not understood (34, 40).

The recent elucidation of the peptide sequences that signal GPI addition has led to the generation of several engineered GPI-anchored proteins (6, 9, 16, 25, 28, 31, 32, 46). GPI-anchored chimeras including the heterodimeric T cell receptor and MHC class II polypeptides, the trimeric VSV G glycoprotein, and the tetrameric *Torpedo* acetycholinesterase all form the same oligomers as their transmembrane-anchored counterparts (9, 16, 31, 46). The PI-PLC-released ectodomains of GPI-anchored T cell receptor, MHC class II, and acetycholinesterase remain as correct oligomers, but detailed knowledge of their structures and functions is lacking (16, 31, 46).

To gain insight into the influence that a GPI anchor can have on the structure and function of an oligomeric membrane protein, we attached a GPI anchor to the well-characterized influenza HA. We then studied GPI-HA's oligomeric state, rate and efficiency of transport to the cell surface, post-translational modifications, receptor binding activity, lateral mobility, conformational changes under fusion-inducing conditions, and, in a separate study (manuscript in preparation), its membrane fusion activity. We show, for the first time, that the structure of a GPI-anchored protein can differ, in a functionally significant manner, from its transmembrane-bound counterpart.

Materials and Methods

Cells and Reagents

All amino acid numbers for X:31 HA correspond to Ward and Dopheide (43). The nucleotide sequences encoding the X:31 HA ectodomain, excised by ClaI and BamHI digestion of the plasmid p72HR (a gift of P. Bates, University of California, San Francisco), and Decay Accelerating Factor (DAF) flanked by EcoRI sites (gift of D. Littman, University of California, San Francisco), were inserted into the corresponding restriction sites of pKSII+ (Stratagene Corp., San Diego, CA) such that the open reading frames were in the same orientation, yielding pHADAF. The sequences between the desired portions of HA and DAF were deleted by standard mutagenesis procedures of pHADAF with either the oligonucleotide DAFHA.TM (5'-GTCTGGATACAAAGACCCAAATAAAGGAAGTGG-3') or DAFHA.BHA (5'-CGGTTTCAGATCAAAGGTCCAAATAAAGGAAGTGG-3') (UCSF BioMolecular Resource Center, San Francisco, CA) (29). These oligonucleotides appended the nucleotide sequence encoding the carboxy terminal 37 amino acids of DAF to the nucleotide sequences encoding the HA ectodomain. The junctions were placed at either the predicted point of membrane insertion (amino acid 184 of HA2) or the bromelain cleavage site (amino acid 175 of HA2) to generate the plasmids pGPI-HA and pGPI-BHA. Chimeras were confirmed by DNA sequence analysis with Sequenase 2.0 (US Biochemical Corp., Cleveland, OH). Sequences encoding GPI-HA and GPI-BHA were isolated by digestion of pGPI-HA and pGPI-BHA with EcoRV and XbaI and ligated into XbaI-SmaI digested pEE14 to yield pGSGPI-HA and pGSGPI-BHA (1). The nucleotide sequence encoding the entire HA coding region was excised from the plasmid pSVX38 (gift of M.-J. Gething, University of Texas, Dallas) by digestion with ClaI and SalI and inserted into ClaI and SalI digested pKSII+ (Stratagene Corp.) yielding the plasmid, pHA. The nucleotide coding sequence of wild-type (wt)-HA, obtained by XbaI-SalI digestion of pHA and filling in the SalI site with the enzyme Klenow, was inserted into XbaI-SmaI digested pEE14 to yield pEEHA (gift of T. Danieli, University of California, San Francisco).

CHO-K1 cells (American Type Culture Collection, Bethesda, MD, CCL 61) were transfected using the standard $CaPO_4$ technique. Cells were grown for 10 d in glutamine deficient minimal essential media (GIBCO BRL, Gaithersburg, MD) containing 10% supplemented calf serum (Hyclone, Logan, UT) and 25 μM methionine sulfoximine (MSX, Sigma Chemical Co., St. Louis, MO) as described (1). Individual colonies were isolated, expanded and replated at a density of 10^6 cells/10-cm dish in the presence of 400 μM MSX. After 10–14 d, individual clones were reisolated and grown continuously in the presence of 400 μM MSX. Cell lines expressing a large amount of either wt-HA, GPI-HA, or GPI-BHA were chosen for further study.

Cell Surface and Metabolic Labeling

Total cell surface proteins were labeled with an amine reactive biotin reagent. Cells grown to confluency in 10-cm dishes were rinsed twice with ice cold PBS pH 7.8 and labeled in 3 ml of PBS, 1 mg/ml immunopure NHS-LC-biotin (Pierce Biochemicals, Rockford, IL), pH 7.8 for 45 min at 4°C. Excess reagent was quenched with two to three washes of ice cold PBS, 50 mM glycine, pH 7.8. After immunoprecipitation, the biotinylated proteins were transferred to nitrocellulose (Schleicher and Schuell, Inc., Keene, NH). The filters were blocked with PBS, 1% skim milk, 10% glycerol, 3% BSA, 1 M glucose, 0.5% Tween-20 and incubated with 0.5 ng/ml of streptavidin-HRP (Pierce Biochemicals) in PBS, 0.1% Tween-20 for 60 min at room temperature. The filters were washed three times in PBS, 0.5% Tween-20 and developed with the Enhanced Chemiluminescence reagent (Amersham Corp., Arlington Heights, IL) according to the manufacturer's instructions.

Proteins were metabolically labeled by incubating cells in media lacking cysteine and methionine (cys^-/met^- MEM Select Amine) (GIBCO BRL) for 30 to 45 min at 37°C. This media was removed and replaced by cys^-/met^- media containing the indicated amount of [^{35}S]TransLabel (ICN, Irvine, CA) and 2% supplemented calf serum. The cells were incubated for 14 to 18 h at 37°C unless otherwise indicated before harvesting.

Immunoprecipitation

Cells expressing either wt-HA or GPI-HA were washed twice in PBS, and lysed on ice for 30 min in lysis buffer (1% NP-40, 100 mM Tris, 1 mM PMSF, 1 μg/ml pepstatin A, 2 μg/ml leupeptin, 4 μg/ml aprotinin, 10 μg/ml antipain, 50 μg/ml benzamidine, 10 μg/ml soybean trypsin inhibitor (STI), 0.5 mM iodoacetamide (IAA) (pH 7.5). The lysate was centrifuged at 15,000 *g* in an Eppendorf microfuge for 20 min. The sample was incubated with 1 μg/ml of the site A mAb (gift of J. Skehel, Medical Research Council, Mill Hill, England) for 60 min at room temperature. The antibody-HA complexes were precipitated with protein A agarose (Schleicher and Schuell, Keene, NH) for 60 min at RT and washed extensively as described (27).

Pulse Chase Analysis

Approximately 10^6 cells were incubated for 30 min at 37°C in cys^-/met^- media. After this preincubation, the cells were pulse labeled for 8 min at 37°C with 100 μCi of [^{35}S]TransLabel in cys^-/met^- media. The chase period was initiated by replacing the cys^-/met^- medium with cys^-/met^- medium containing an excess of nonradioactive cysteine and methionine for the indicated period of time at 37°C. During the final 8 min of chase, trypsin was added to a final concentration of 10 μg/ml at 37°C. Cells were then placed on ice and STI was added to 100 μg/ml. Samples were then processed by the addition of 0.1 vol of 10× lysis buffer to the media and mixing. The resulting material was collected, incubated on ice for 30 min and centrifuged for 30 min at 15,000 *g* in an Eppendorf microfuge. The resulting supernatant was immunoprecipitated.

PI-PLC Treatment

Cells were rinsed twice with PBS and incubated in PBS, 10 μg/ml BSA, 100 mU/ml PI-PLC (Boehringer-Mannheim Corp., Indianapolis, IN).

Fluorescence Photobleaching Recovery (FPR) Analysis

Polyclonal rabbit antiserum raised against virions of the X:31 strain was

used throughout. Monovalent Fab' fragments labeled with TRITC (Molecular Probes, Inc., Eugene, OR) were prepared from the IgG fraction as described following standard labeling procedures (19). The Fab' preparation was free of contamination by $F(ab')_2$ or IgG, as judged by SDS-PAGE under nonreducing conditions. The use of monovalent antibody fragments eliminates the possibility of IgG mediated cross-linking.

Lateral diffusion coefficient (D) and mobile fractions (R_f) of wt-HA and GPI-HA on the surface of CHO cells were measured by FPR, using an apparatus described previously (19). Cells were split and grown on glass coverslips 2 d before the experiment. They were washed twice in Hank's balanced salt solution with Earle's salts (HBSS; Beth Haemek, Israel), supplemented with 20 mM Hepes and 2% BSA (HBSS/Hepes/BSA, pH 7.2), and incubated with anti-HA TRITC-Fab' (100 μg/ml, 60 min, 4°C). Alternatively, they were labeled with the fluorescent lipid probe *N*-4-nitrobenzo-2-oxa-1,3-diazolyl-phosphatidylethanolamine (*N*-NBD-PE, Avanti Polar Lipids, Inc., Pelham, AL) in HBSS/Hepes (devoid of BSA) as described earlier (19). After rinsing three times, the coverslips were placed (cells facing downward) over a serological slide with a depression filled with the same buffer equilibrated at the desired temperature (37 or 22°C). A thermostated microscope stage was used to keep the sample temperature constant throughout the FPR experiment, performed within 45 min of labeling. The monitoring laser beam (529.5 nm, 1 μW, for TRITC; 488 nm, 0.1 μW, for *N*-NBD-PE) was focused through the microscope (Zeiss Universal) to a Gaussian radius of (0.61 +/− 0.02) μm with an ×100 oil immersion objective. A brief pulse (5 mW, 30 ms, for TRITC; 0.5 mW, 60 ms for *N*-NBD-PE) bleached 50–70% of the fluorescence in the illuminated region. The time course of fluorescence recovery was followed by the attenuated monitoring beam. D and R_f were extracted from the fluorescence recovery curves by nonlinear regression analysis (19). Incomplete recovery was interpreted to represent fluorophores that are immobile on the FPR experimental time scale ($D \leq 5 \times 10^{-12}$ cm²/s).

Cell Surface Cross-linking

Approximately 10^6 cells were labeled with 250 μCi of [^{35}S]TransLabel for 16 h, washed twice with HBS (10 mM Hepes, 150 mM NaCl, pH 8.0) and incubated with the indicated concentration of 3,3'-dithio*bis*(sulfosuccinimidylpropionate) (DTSSP, Pierce Chemical Co., Rockford, IL) for 45 min at room temperature. Excess reagent was quenched by washing two times with HBS/50 mM glycine. The cells were washed one time with HBS and lysed by the addition of lysis buffer. After immunoprecipitation, the immunecomplexes were suspended in 62.5 mM Tris pH 7.5, 2% SDS, 7.5% sucrose, 0.5 mM EDTA, 0.005% bromophenol blue (loading buffer), heated to 95°C for 5 min, separated on nonreducing 5% SDS-PAGE and fluorographed with Amplify (Amersham Corp.).

Gradient Analysis of BHA, and PI-PLC-released GPI-HA and GPI-BHA

Six T-175 flasks of cells expressing either wt-HA or GPI-HA and four T-175 flasks of cells expressing GPI-BHA were metabolically labeled with 0.4 mCi/flask of [^{35}S]TransLabel for 16 h. The cells were incubated with 5 μg/ml trypsin-TPCK (Sigma Chemical Co.) in RPMI-1640 for 5 min at room temperature. The cleavage reaction was inhibited by the addition of 50 μg/ml STI in RPMI-1640. The cells were washed twice in PBS/0.5 mM EDTA/0.5 mM EGTA, incubated in the same solution for 10 min at room temperature, and collected by centrifugation at 115 *g* for 5 min. For BHA preparations, the cells were lysed for 30 min on ice in lysis buffer. After centrifugation in a TLA100.3 rotor (Beckman Instruments, Fullerton, CA) at 70,000 *g* for 30 min at 4°C, 2 betamercaptoethanol and bromelain were added to the lysate to final concentrations of 20 mM and 0.1 mg/ml, respectively. Digestion proceeded for 6 h at 37°C and was inhibited by the addition of 100 mM *n*-ethylmaleimide and the proteinase inhibitor cocktail described above. The ectodomains of GPI-HA and GPI-BHA were released from intact cells by PI-PLC digestion as described above. BHA, PI-PLC-released GPI-HA, and PI-PLC-released GPI-BHA were purified by ricin sepharose chromatography as described (48). The purified material was then applied to a continuous gradient of 5–25% sucrose in 30 mM MES, 150 mM NaCl, pH 7.0. The samples were centrifuged at 200,000 *g* for 16 h at 4°C in an SW-41 rotor (Beckman Instruments). Fractions were collected from the bottom of the tube and prepared for scintillation counting.

Peptide N-Glycosidase F Digestion

Approximately 10^6 cells expressing either wt-HA or GPI-HA were incubated with 50 μCi of [^{35}S]TransLabel for 16 h. Cells were rinsed twice with PBS and lysed with lysis buffer. The lysates were digested with 10 μg/ml of trypsin-TPCK for 30 min at room temperature; inhibition was terminated by the addition of 100 μg/ml STI and the protease inhibitors described above. HA was immunoprecipitated, the immunecomplexes were boiled in a solution containing 1% octylglucoside, 0.1% SDS, 20 mM Tris pH 8.3, 10 mM EDTA, 1% BME for 10 min at 95°C, the sepharose beads were removed by centrifugation at 15,000 *g* for 10 s, and the supernatant was aliquoted. After cooling to room temperature, 1 μl of Peptide *N*-glycosidase F (Boehringer-Mannheim Corp.) was added and the proteins digested for 16 h at 37°C. An additional 1 μl of Peptide *N*-glycosidase F was added and incubation continued for 7 h at 37°C. After addition of an equivalent amount of 2× sample buffer containing 100 mM DTT, samples were heated to 95°C for 5 min and separated by 12% SDS-PAGE.

DMM Treatment of Cells

Approximately 10^6 cells expressing either wt-HA or GPI-HA were labeled with 100 μCi of [^{35}S]TransLabel in the presence of 0.5 mM dMM (CalBiochem, San Diego, CA) for 2 h at 37°C. After 2 h the cys^-/met^- medium was replaced with cys^-/met^- medium containing excess cysteine and methionine and 0.5 mM dMM for 2 h. The cells were briefly trypsinized with 5 μg/ml of trypsin for 5 min and lysed. Wt-HA and GPI-HA were immunoprecipitated and separated by 10% SDS-PAGE. The gel was fluorographed with Entensify (New England Nuclear, Boston, MA).

Red Cell Binding

To analyze the receptor binding activity of HA, cells expressing either wt- or GPI-forms of HA were grown for 48 h in the presence or absence of 0.25 mM dMM as indicated. Confluent monolayers were treated with 5 μg/ml trypsin-TPCK and 0.2 mg/ml neuraminidase (Sigma Chemical Co.) for 10 min at room temperature. The cells were washed twice with RPMI-1640 and incubated with an 0.05% suspension of washed human erythrocytes labeled with octadecylrhodamine (R_{18}) as described (27) for 10 min at room temperature. Unbound RBCs were removed by six washes with RPMI-1640, and the cells were photographed.

Proteinase K (PK) Digestion

Cells expressing GPI-HA or wt-HA were metabolically labeled with [^{35}S]TransLabel for 16 h in the presence or absence of 0.25 mM dMM. The cells were briefly trypsinized with 5 μg/ml of trypsin-TPCK for 5 min at room temperature and removed from their dishes with PBS, 0.5 mM EDTA, 0.5 mM EGTA. The ectodomain of GPI-HA was released by digestion with PI-PLC as described above. BHA was produced with bromelain that had been pretreated with reducing agent: 10 mg/ml bromelain was treated with 2 mM DTT for 10 min and the DTT removed by Sepharose G-25 filtration in an argon atmosphere. DTT-treated bromelain (0.1 mg/ml final concentration) was then added to a suspension of intact wt-HA expressing cells through which argon had been bubbled and incubation continued for 16 h at 37°C. Digestion was inhibited by the addition of 100 mM NEM and 10 μg/ml BSA followed by two successive centrifugations at 15,000 *g* in an Eppendorf microfuge. Aliquots of ^{35}S-labeled BHA and PI-PLC-released GPI-HA in MES-saline pH 7.0 were lowered to the indicated pH value by the addition of a predetermined amount of 0.1 M citric acid and incubated for 15 min at 37°C. The samples were reneutralized by the addition of a predetermined amount of 1.0 M Tris base. $CaCl_2$ and PK were added to 2 mM and 0.2 mg/ml, respectively, and incubation continued for 30 min at 37°C. The digestion was stopped by the addition of 1 μg BSA, 1 mM PMSF, and proteinase inhibitors. The proteins were immunoprecipitated with the site A mAb, separated by 10% SDS-PAGE and visualized by fluorography following treatment with Entensify.

Triton X-114 Partitioning

Approximately 5×10^7 cells expressing either wt-HA or GPI-HA were labeled with 3.0 mCi of [^{35}S]TransLabel for 18 h at 37°C. PI-PLC-released GPI-HA and BHA were prepared as described above. The ^{35}S-labeled polypeptides were applied to a matrix of the site A mAb covalently cross-linked to protein A agarose (24). The unbound material was discarded and the column washed with 20 vol each of 12.5 mM potassium phosphate, pH 7.4; 600 mM NaCl, 12.5 mM potassium phosphate, 300 mM NaCl, pH 7.4; and 10 mM potassium phosphate pH 8.0. The bound protein was eluted with 100 mM triethylamine and immediately neutralized by the addition of 1 M potassium phosphate. The material was dialyzed overnight against Mes-saline at 4°C. Purified BHA or PI-PLC-released GPI-HA was in-

cubated at pH 7.0 or 5.2 for 15 min at 37°C, reneutralized, and subjected to TX-114 partitioning by the method of Bordier (13). The aqueous and detergent phases were separated and immunoprecipitated with the polyclonal anti-HA serum. Immunecomplexes were boiled, reduced and separated by 10% SDS-PAGE.

Sucrose Gradient Sedimentation of Cell Surface HA

Cell surface proteins were trypsinized with 5 μg/ml trypsin for 5 min at room temperature and biotinylated. After biotinylation, the cells were removed from their dishes by incubation with PBS/0.5 mM EDTA/0.5 mM EGTA. The cells were resuspended in 1.0 ml MES-saline and aliquoted. One aliquot was lowered to pH 5.2 by the addition of 0.1 M citric acid and incubated for 10 min at 37°C. The cells were reneutralized, washed and lysed in lysis buffer. The lysates were clarified by centrifugation at 70,000 *g* in a TLA 100.3 rotor for 30 min at 4°C. The supernatants were applied to a 5–25% sucrose gradient containing 0.1% NP40 in MES-saline. 14 fractions were recovered, immunoprecipitated with the site A mAb, and separated by 10% SDS-PAGE. The proteins were transferred to nitrocellulose, probed with streptavidin-HRP conjugate and developed with enhanced chemiluminescence.

Results

Construction of GPI-anchored HA

To evaluate the influence of a GPI anchor on the ectodomain of a type I integral membrane glycoprotein, we constructed GPI-anchored forms of the well-characterized influenza HA. Replacement of the normal transmembrane and cytoplasmic domains of several other type I integral membrane glycoproteins with the carboxy terminal 37 amino acids of DAF confers GPI anchor addition (6, 28, 31). We constructed GPI-HA and GPI-BHA (Fig. 1) by appending this 37 amino acid signal to sequences encoding the HA ectodomain at either the transmembrane junction (amino acid 184 of HA2; GPI-HA) or at the bromelain cleavage site (amino acid 175 of HA2; GPI-BHA). GPI-HA, which has the GPI anchor added at the point of predicted membrane insertion, is analogous to other GPI-anchored chimeras (6, 9, 16, 25, 28, 31, 32, 46). GPI-HBA was constructed because its ectodomain would be analogous to the highly characterized BHA molecule (49). Because GPI-HA contains the complete HA ectodomain, it was characterized in greater detail; however, both polypeptides behaved identically in all assays. CHO cells that stably express high levels of GPI-HA, GPI-BHA, and wt-HA were isolated as described in Materials and Methods.

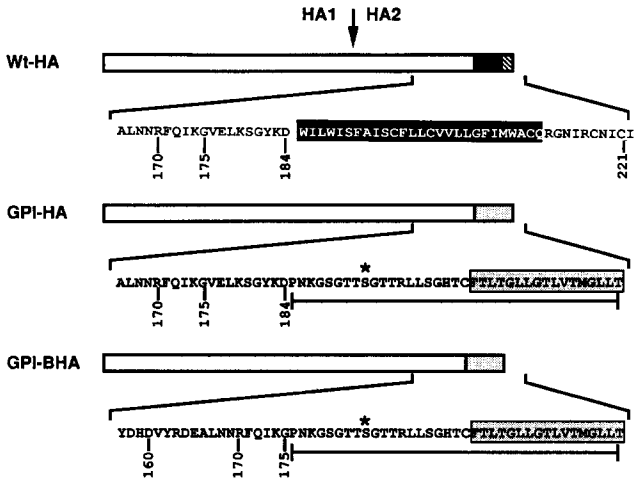

Figure 1. Structure of the GPI-HA and GPI-BHA chimeras. The top diagram depicts wt-HA: the ectodomain (□), transmembrane polypeptide (■), and cytoplasmic domain (▨) are indicated. The arrow marks the position of the HA1-HA2 proteolytic cleavage site. The middle and bottom diagrams depict the GPI-(B)HA chimeras, indicating the relative location of the hydrophobic region of DAF (▩). The amino acid sequence beneath each diagram identifies the junction between the HA ectodomain and either the HA transmembrane (*white letters*; *wt-HA*) or the 37 amino acid GPI-anchor addition sequence from DAF (*bar under sequences*; *GPI-HA*, *GPI-BHA*). The numbers refer to the amino acid position in the HA2 subunit (43). The asterisk over the Ser in the DAF indicates the predicted point of attachment for the GPI anchor (32).

Expression and Transport of GPI-HA to the Cell Surface

We first tested whether GPI-HA and GPI-BHA are transported to the cell surface. CHO cells do not proteolytically process the nonfusogenic HA0 into the disulfide-linked HA1 and HA2 subunits (23, 27). We therefore determined the amount of HA transported to the cell surface using a trypsin-sensitivity assay (7). Cells expressing either GPI-HA, GPI-BHA or wt-HA were metabolically labeled with [^{35}S]Trans-Label for 18 h, briefly trypsinized, and lysed. The lysates were immunoprecipitated with an anti-HA mAb and separated by SDS-PAGE (Fig. 2 *a*). The GPI-anchored forms, like wt-HA, were produced as the HA0 precursor (Fig. 2 *a*, lanes without trypsin). Phosphorimager analysis indicated that, upon addition of exogenous trypsin, ~85% of total cellular wt-HA0, GPI-HA0 and GPI-BHA0 were cleaved into their HA1 and HA2 polypeptide chains (Fig. 2 *a*, lanes plus trypsin), and that roughly equivalent amounts of wt-HA, GPI-HA and GPI-BHA were expressed at the cell surface. Indirect immunofluorescence of nonpermeabilized cells confirmed the cell surface localization of GPI-HA and GPI-BHA (data not shown). These results indicated that GPI-HA0 and GPI-BHA0 reach the cell surface efficiently and can be cleaved to generate the HA1 and HA2 polypeptides.

The HA0, HA1, and HA2 polypeptide chains of the GPI-anchored HAs migrated differently than their wt counterparts on SDS gels (Fig. 2 *a*). The estimated molecular weights of GPI-HA2 and GPI-BHA2 were consistent with carboxy terminal processing and GPI anchor addition (32). The slower migration of GPI-HA2 relative to GPI-BHA2 (Figs. 1 and 2 *a*) is consistent with the 9 amino acid difference between GPI-HA2 and GPI-BHA2. However, the slower migration of GPI-HA1 and GPI-BHA1 (relative to HA1) could not be accounted for by differences in protein mass, because these subunits have identical primary structures (Fig. 1). Posttranslational modifications, specifically terminal glycosylation, slowed the migration of GPI-HA1 and GPI-BHA1 relative to HA1 (see below).

We next tested whether the GPI anchor altered the rate of transport of the HA ectodomain through the constitutive secretory pathway. Cells expressing either wt-HA or GPI-HA were pulse labeled with [^{35}S]cysteine and methionine for 10 min and chased for various intervals (Fig. 2 *b*). During the last 8 min of the chase trypsin was added to convert cell surface wt-HA0 and GPI-HA0 to their disulfide-linked subunits. The approximate t1/2 for appearance of both wt HA and GPI-HA at the cell surface was 50 min and both mol

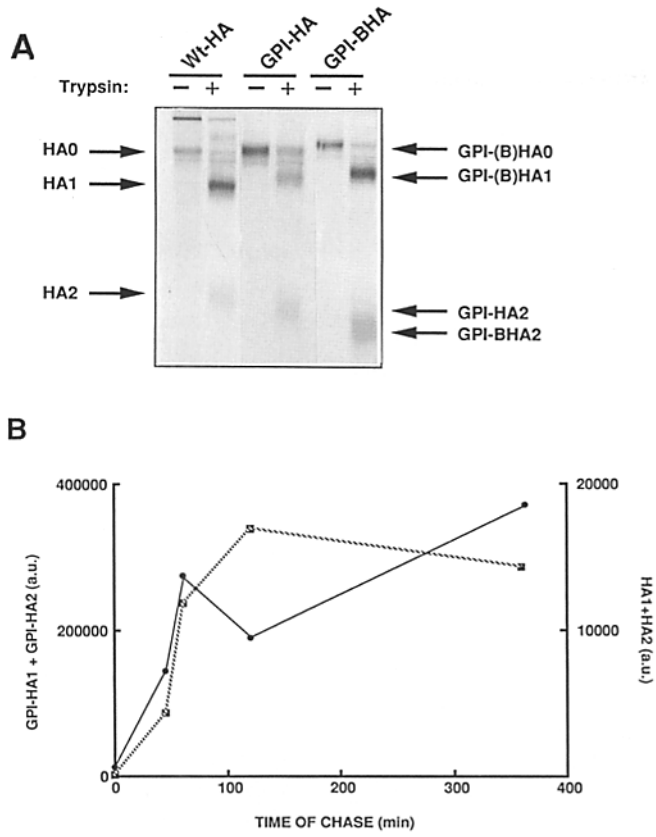

Figure 2. Transport of GPI-HA and GPI-BHA to the cell surface. (*A*) Transport to the cell surface was assessed by trypsinization of intact cells. Cells expressing either wt-HA, GPI-HA, or GPI-BHA were labeled with [^{35}S] for 18 h then treated with 10 μg/ml trypsin (+) or STI (−) for 10 min at room temperature. Equivalent amounts of each lysate were immunoprecipitated with the site A mAb, separated by SDS 10% PAGE, and autoradiographed. The arrows on the left indicate the positions of the wt-HA subunits and the arrows on the right mark the positions of the GPI-(B)HA subunits. (*B*) Pulse chase analysis of wt-HA and GPI-HA in CHO derived cell lines. Cells expressing either wt-HA (*circles*; *solid line*) or GPI-HA (*squares*; *hashed line*) were pulsed for 8 min with 100 μCi of [^{35}S]TransLabel. The chase was initiated by replacing the [^{35}S] containing media with media containing an excess of cysteine and methionine. During the final 8 min of the chase period, trypsin was added to 10 μg/ml to cleave cell surface HA. STI was added, total HA immunoprecipitated, boiled, reduced, and separated by 10% SDS-PAGE. The autoradiogram was quantitated by phosphorimager analysis and the amount of HA1 and HA2 (*a.u.*, *arbitrary units*) is plotted with respect to the time of chase.

ecules were stable for at least 6 h. GPI-HA is therefore transported to the cell surface with approximately the same rate and efficiency as wt-HA (Fig. 2).

Membrane Attachment of GPI-HA

We predicated that GPI-HA and GPI-BHA would be anchored in the membrane by a GPI moiety (6, 31). To test this prediction we treated intact biotinylated cells with PI-PLC (18). The media and cells were then immunoprecipitated with an anti-HA antibody and probed with streptavidin-HRP (Fig. 3). Wt-HA was exclusively associated with the cell pellet whether it was or was not treated with PI-PLC (Fig. 3, lanes *1–4*). In the absence of PI-PLC, GPI-HA and GPI-BHA remained with the cell pellet (Fig. 3, lanes *5, 6, 9, 10*). However, PI-PLC released a large proportion of GPI-HA and GPI-BHA into the supernatant (Fig. 3, lanes *7, 8, 11, 12*). The GPI-HA and GPI-BHA remaining with the cell pellet after PI-PLC treatment may contain modifications that render the GPI anchor resistant to PI-PLC (42). These findings demonstrated that GPI-HA and GPI-BHA are anchored to the membrane via a GPI moiety, and that their ectodomains can be released by digestion with PI-PLC.

Lateral Mobility of GPI-anchored HA

Where studied, GPI-anchored proteins diffuse approximately two times faster than their transmembrane-anchored counterparts (52). The lateral diffusion coefficient of GPI-HA was 10×10^{-10} cm^2/s at 37°C (Table I) compared to 5×10^{-10} cm^2/s for wt-HA, consistent with previous findings on wt-HA from a different influenza virus strain (19). Approximately 65% of GPI-HA was mobile, similar to wt-HA (Table I). Thus, like other GPI-linked proteins, GPI-HA diffuses twofold more rapidly than transmembrane-anchored HA (52). The high R_f values which are close to those observed for a phospholipid probe under the same conditions (Table I), indicated that GPI-anchored HA diffuses freely in the membrane, and is not segregated into specialized membrane domains (17).

Oligomeric Form of GPI-anchored HA on the Cell Surface

Improperly folded or oligomerized forms of HA do not reach the cell surface (7, 22, 37). Because GPI-HA is transported to the cell surface (Fig. 2), it is likely a trimer. To test this prediction, cells expressing wt-HA or GPI-HA were metabolically labeled and cross-linked with the membrane impermeable crosslinker, DTSSP. Cell lysates were prepared,

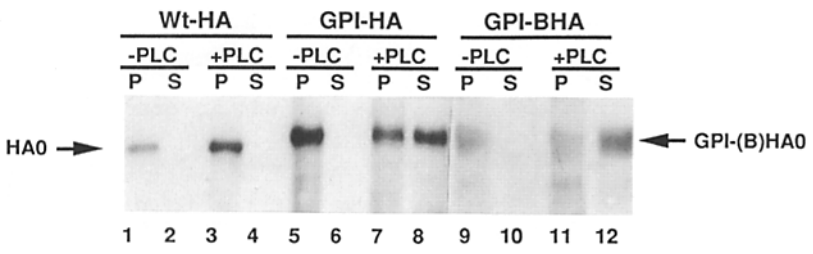

Figure 3. PI-PLC release of GPI-HA and GPI-BHA from the cell surface. Cells expressing either wt-HA or GPI-HA were biotinylated and the intact cells were treated with (+*PLC*) or without (−*PLC*) PI-PLC for 60 min at 37°C. The media (*S*) and cell pellets (*P*) were harvested separately and prepared for immunoprecipitation with the site A mAb. The immunecomplexes were reduced, separated on SDS 10% PAGE, probed with streptavidin-HRP and developed with ECL. The position of HA0 and GPI-HA0 are indicated.

Table I. Lateral diffusion of wt-HA and GPI-HA in CHO Cells

Membrane component labeled	Temperature	D × 10^{-10}	R_f
	°C	cm^2/s	
wt-HA	37	4.9 ± 0.4	75 ± 3
	22	1.9 ± 0.3	70 ± 6
GPI-HA	37	9.9 ± 1.1	67 ± 3
	22	2.5 ± 0.3	64 ± 5
N-NBD-PE	37	43 ± 4	80 ± 3
	22	21 ± 2	77 ± 5

CHO cells expressing wt-HA and GPI-HA were prepared for lateral mobility measurements as described in Materials and Methods.

immunoprecipitated with an anti-HA antibody, and separated on nonreducing 5% SDS polyacrylamide gels (Fig. 4). In the absence of cross-linker, wt-HA migrated as three distinct species corresponding to monomer, dimer and trimer (Fig. 4, lane *1*). Interactions among the transmembrane and cytoplasmic domains account for the association of wt-HA monomers on nonreducing SDS-gels. BHA, which lacks the transmembrane and cytoplasmic domains, migrates completely as a monomer on nonreducing SDS gels (see 12 and Fig. 5 *a*, *inset*). Addition of 10 mM DTSSP to wt-HA increased the proportion of the trimer band (Fig. 4, lane *2*). In the absence of cross-linker, GPI-HA migrated completely as a monomer (Fig. 4, lane *3*). Upon addition of DTSSP, however, a band corresponding to a GPI-HA trimer, and a weaker band corresponding to a GPI-HA dimer (see also Fig. 5 *b*), appeared (Fig. 4, lane *4*). Moreover, cell surface GPI-HA cosedimented with 9S trimers of wt-HA on 5–25% sucrose gradients (see Fig. 10). These analyses indicated that GPI-HA is present at the cell surface as a 9S trimer. Unlike transmembrane-anchored HA, but identical to BHA, the GPI-HA trimer is not stable in SDS.

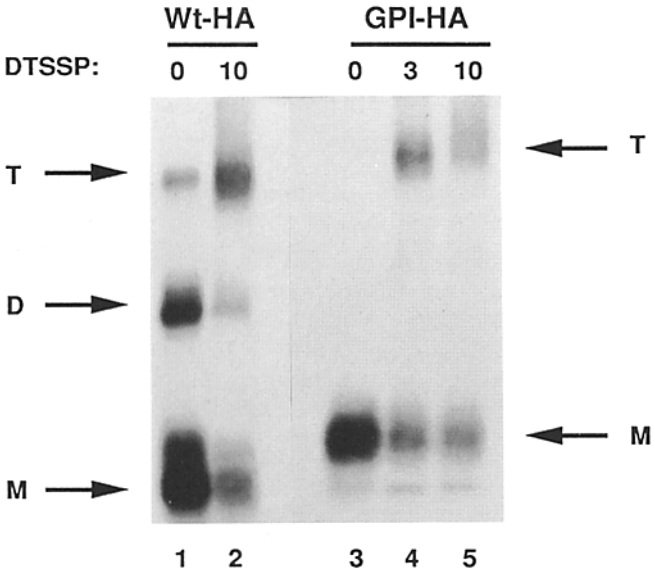

Figure 4. Oligomeric form of GPI-HA on the cell surface. (*A*) Cell surface cross-linking of intact cells. Cells expressing either wt-HA or GPI-HA were labeled with [^{35}S]TransLabel for 18 h at 37°C and treated with the indicated concentration of DTSSP for 45 min at room temperature. After quenching excess reagent, the cells were lysed, and immunoprecipitated with the site A mAb. The immunecomplexes were boiled in the presence of SDS and separated by nonreducing 5% SDS-PAGE. The position of the trimeric (*T*), dimeric (*D*) and monomeric (*M*) forms are indicated.

Oligomeric Form of GPI-HA Released with PI-PLC

The water soluble ectodomain of wt-HA prepared with bromelain, BHA, retains the oligomeric structure of membrane-bound HA (47, 49). To establish the oligomeric structure of PI-PLC-released GPI-HA, cells expressing wt-HA, GPI-HA, or GPI-BHA were metabolically labeled, treated with bromelain or PI-PLC, and separated on 5–25% sucrose gradients. PI-PLC-released GPI-HA and GPI-BHA cosedimented with 9S BHA trimers (Fig. 5). The presence or absence of nonionic detergent did not change these sedimentation profiles (data not shown). A sample of the peak fraction (No. 11) from the BHA and PI-PLC-released GPI-HA and GPI-BHA gradients was removed and cross-linked with DTSSP. As shown in Fig. 5 (*insets*), both BHA and PI-PLC-released GPI-(B)HA migrated as monomers on nonreducing SDS gels (12). Upon addition of DTSSP, however, dimeric and trimeric forms of BHA and PI-PLC-released GPI-(B)HA were detected (Fig. 5, *insets*). Therefore, both sedimentation and cross-linking analyses indicated that GPI-(B)HA, like BHA, remains trimeric after release from its membrane anchor.

The Ectodomain of GPI-HA Contains Additional Oligosaccharides

BHA contains seven *N*-linked oligosaccharide chains, six on the HA1 subunit. Two of the oligosaccharide chains, attached to asparagine residues HA1 165 and HA1 285 retain the high mannose form (50). GPI-HA1 and GPI-BHA1 migrated slower than wt-HA1 in SDS-PAGE (see Fig. 2 *a* and Fig. 6 *a*). To test whether additional oligosaccharide processing accounted for this slower mobility, we treated GPI-HA, GPI-BHA and wt-HA with Peptide *N*-glycosidase F to remove *N*-linked oligosaccharide chains. After this treatment the core polypeptides of all HA1 subunits migrated identically (Fig. 6 *a*). Consistent with this observation, GPI-HA1 and GPI-BHA1 were completely resistant, unlike wt-HA1, to digestion with EndoH (data not shown), indicating that GPI-anchored HA1 subunits do not contain any high mannose oligosaccharide chains. Thus, GPI-HA1 and GPI-BHA1 contain more terminally processed oligosaccharide chains than wt-HA1.

Treatment of cells with dMM inhibits mannosidase I activity, yielding glycoproteins that contain only high mannose oligosaccharide chains (5). dMM treatment of influenza virus-infected cells prevents the addition of complex oligosaccharide chains to (wt-)HA yet has no effect on virus binding or infectivity (5). Wt-HA-expressing cells were grown in the presence of dMM and labeled with [^{35}S]TransLabel. After brief trypsinization and immunoprecipitation, we found that the wt-HA1 subunit from cells grown in the presence of dMM migrated faster than wt-HA1 from cells grown in normal media (Fig. 6 *b*). In a similar manner, growth of GPI-HA-expressing cells in medium containing dMM pro-

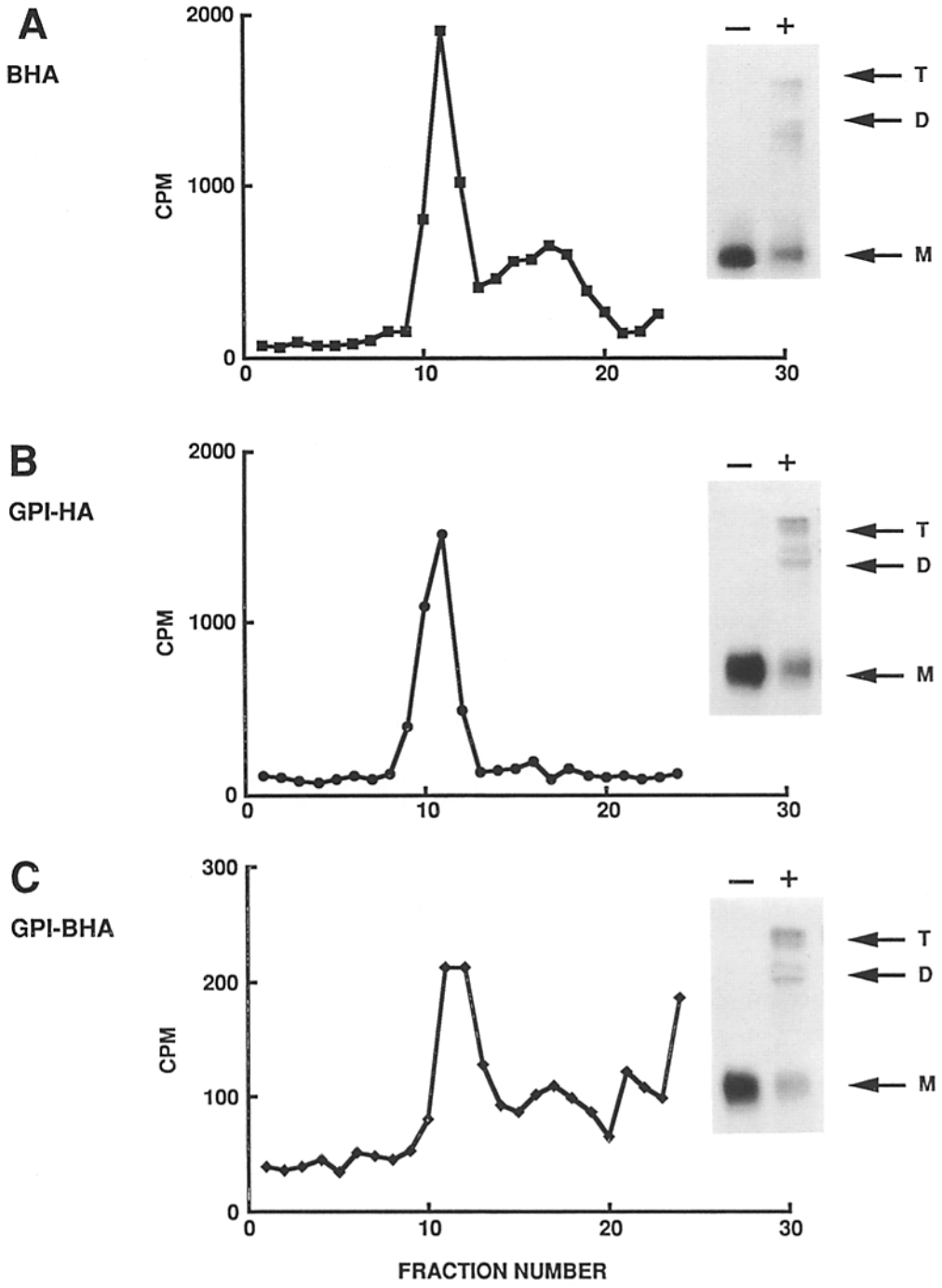

Figure 5. Oligomeric form of PI-PLC-released GPI-HA and GPI-BHA. Gradient analysis of BHA and PI-PLC-released GPI-HA and GPI-BHA. Cells expressing wt-HA (*A*), GPI-HA (*B*), and GPI-BHA (*C*) were labeled with [^{35}S]Trans-Label for 20 h, briefly trypsinized and harvested. Cells expressing wt-HA were treated with bromelain as described and cells expressing GPI-(B)HA were digested with PI-PLC for 60 min at 37°C. The released material was affinity purified on ricin sepharose and applied to a 5–25% sucrose gradient. After sedimentation, fractions were collected and monitored by scintillation counting. The cpm for each fraction is plotted with respect to the fraction number. (*Inset*) An aliquot of the peak fraction from each gradient was removed and treated with (+) or without (−) 5 mM DTSSP for 30 min at room temperature. The reaction was quenched and the material immunoprecipitated with the Site A mAb. The immunecomplexes were separated on nonreducing 10% SDS-PAGE and subjected to autoradiography. The position of the monomeric (*M*), dimeric (*D*) and trimeric (*T*) species are indicated.

duced a GPI-HA1 subunit that migrated faster than GPI-HA1 produced in the absence of dMM (Fig. 6 *b*). Importantly however, the GPI-HA1 and wt-HA1 subunits from cells grown in the presence of dMM migrated identically to one another, consistent with the hypothesis that dMM treatment generates glycoproteins containing only high mannose oligosaccharide chains (5). Subsequent EndoH digestion of wt-HA and GPI-HA produced in the presence of dMM confirmed that all of the oligosaccharide chains on HA produced in this manner were in the high mannose form (data not shown). These results demonstrated that GPI-HA1 undergoes additional terminal oligosaccharide processing relative to wt-HA1, specifically to the oligosaccharide chains attached to asparagine HA1 165 and/or HA1 285.

Additional Oligosaccharide Processing of GPI-HA Abolishes Its Ability to Bind Erythrocytes

Wt-HA binds sialic acid residues on the surface of host cell membranes via a receptor binding pocket found near the tip of the HA molecule (44). As shown in Fig. 7, wt-HA-expressing cells bound large numbers of erythrocytes which contain a large amount of sialic acid on their surface. Cells expressing GPI-HA or GPI-BHA, however, did not bind

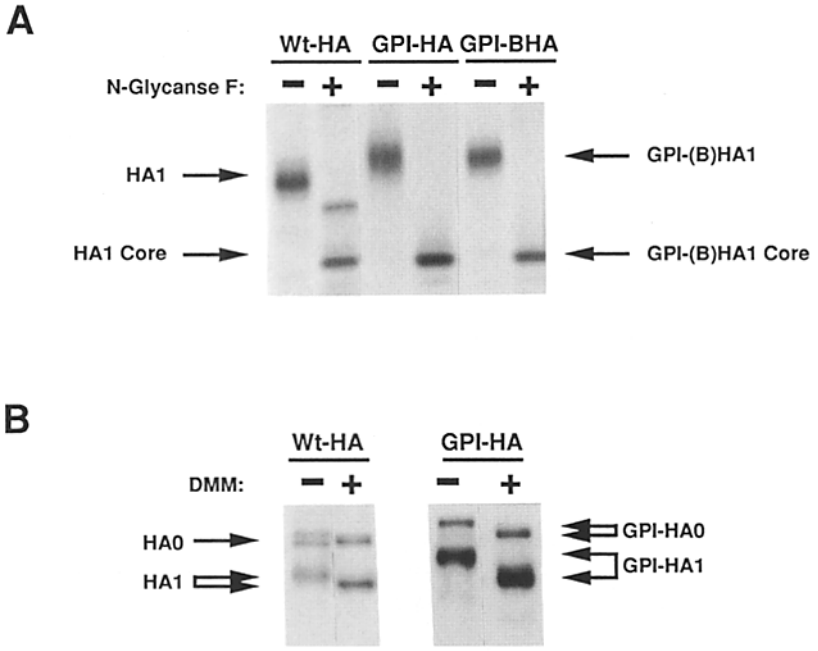

Figure 6. Oligosaccharide modifications to GPI-HA. (*A*) *N* glycanase F digestion of wt-HA, GPI-HA, and GPI-BHA. Cells expressing either wt-HA, GPI-HA, or GPI-BHA were labeled with [^{35}S]TransLabel for 16 h at 37°C, briefly trypsinized, lysed, and the HA precipitated with the site A mAb. The immunecomplexes were boiled, reduced, and digested with *N* glycanase F for 18 h at 37°C. The samples were again boiled, reduced, and separated on 12% SDS-PAGE and fluorographed. The positions of the polypeptides before and after ("Core") *N*-glycanase F digestion are marked. (*B*) Growth of cells in the presence of dMM alters the glycosylation of wt-HA and GPI-HA. Cells expressing wt-HA or GPI-HA were labeled with [^{35}S]TransLabel in the presence (+) or absence (−) of 0.25 mM dMM for 18 h at 37°C. The cells were briefly trypsinized, lysed, and the HA immunoprecipitated. Immunecomplexes were boiled, reduced, separated on 10% SDS-PAGE, and fluorographed. The positions of the polypeptides are marked.

erythrocytes indicating a loss of receptor binding activity (Fig. 7). Because GPI-HA and GPI-BHA contain additional oligosaccharide modifications, which could be prevented by production in the presence of dMM, we tested the ability of dMM-treated HA-expressing cells to bind erythrocytes. Consistent with previous results, wt-HA produced in the presence of dMM bound erythrocytes as well as wt-HA produced in normal medium (Fig. 7) (5). Growth of GPI-HA and GPI-BHA-expressing cells in dMM restored their erythrocyte binding activity (Fig. 7). We conclude, in combination with the preceding analysis, that processing of additional oligosaccharide chains to complex forms abolishes the ability of GPI-HA and GPI-BHA to bind erythrocytes. This defect can be fully alleviated, however, by growth of GPI-(B)HA-expressing cells in dMM.

Low pH-induced Conformational Changes of the GPI-HA Ectodomain

The water soluble BHA ectodomain undergoes characteristic low pH-induced conformational changes like wt-HA (13, 47, 49). We therefore asked whether the GPI-HA ectodomain undergoes these changes. We first measured the pH at which GPI-HA becomes proteinase sensitive. We incubated ^{35}S-labeled BHA or PI-PLC-released GPI-HA at different pH values for 15 min at 37°C, and then reneutralized, digested with Proteinase K (PK), and analyzed the samples on 10% SDS-PAGE (Fig. 8). As shown previously, BHA was not susceptible to degradation by PK unless it was treated below pH 5.4. Growth of cells expressing wt-HA in dMM did not alter this pattern. PI-PLC-released GPI-HA was also resistant to the action of PK at pH 7.0, but it became susceptible below pH 5.8. GPI-BHA behaved similarly (data not shown). PI-PLC-released GPI-HA produced in the presence of dMM became PK sensitive after treatment below pH 5.6. This analysis indicated that, like BHA, PI-PLC-released GPI-HA becomes PK sensitive after exposure to low pH. However, proteinase K sensitivity occurs at 0.4 and 0.2 pH units higher than for BHA when produced in the absence or presence of dMM, respectively. In terms of its pH dependence, GPI-HA behaves like HA mutants that display elevated fusion pH dependencies due to point mutations in the ectodomain (49).

Low pH treatment causes BHA to become hydrophobic (13, 47, 49). We determined whether PI-PLC-released GPI-HA becomes hydrophobic by measuring its ability to partition into the detergent TX-114. ^{35}S-labeled BHA and PI-PLC-released GPI-HA were incubated at pH 7.0 or pH 5.2 for 15 min at 37°C, reneutralized, and extracted with TX-114 (13). The detergent and aqueous phases were separated, adjusted to similar compositions and immunoprecipitated with the anti-HA serum. As shown in Fig. 9, both BHA and PI-PLC-released GPI-HA partitioned into the aqueous phase at neutral pH. After treatment at low pH, however, both BHA and PI-PLC-released GPI-HA partitioned into the detergent phase (Fig. 9). Under these conditions over 90% of the GPI-HA and GPI-BHA (data not shown) partitioned into the detergent phase. These results demonstrated that, like BHA, PI-PLC-released GPI-(B)HA acquires hydrophobic properties after low pH treatment.

Low pH induces hydrophobic properties in BHA due to release of the fusion peptides from the trimer interface (48). We therefore tested whether the fusion peptides are exposed from PI-PLC-released GPI-HA. ^{35}S-labeled BHA and PI-PLC-released GPI-HA were incubated at pH 7.0 or 5.2 for 5 min at 37°C, reneutralized, and incubated with an antiserum to the fusion peptide. As shown in Table II, the neutral pH forms of BHA and PI-PLC-released GPI-HA did not react with the fusion peptide antiserum. After low pH treatment, however, the fusion peptides in both molecules were detected with the anti-fusion peptide antiserum. Conversely, two neutral pH specific epitopes located at the tip of the trimer, whose reactivities are lost concomitant with fusion peptide exposure (27), were only recognized in the neutral

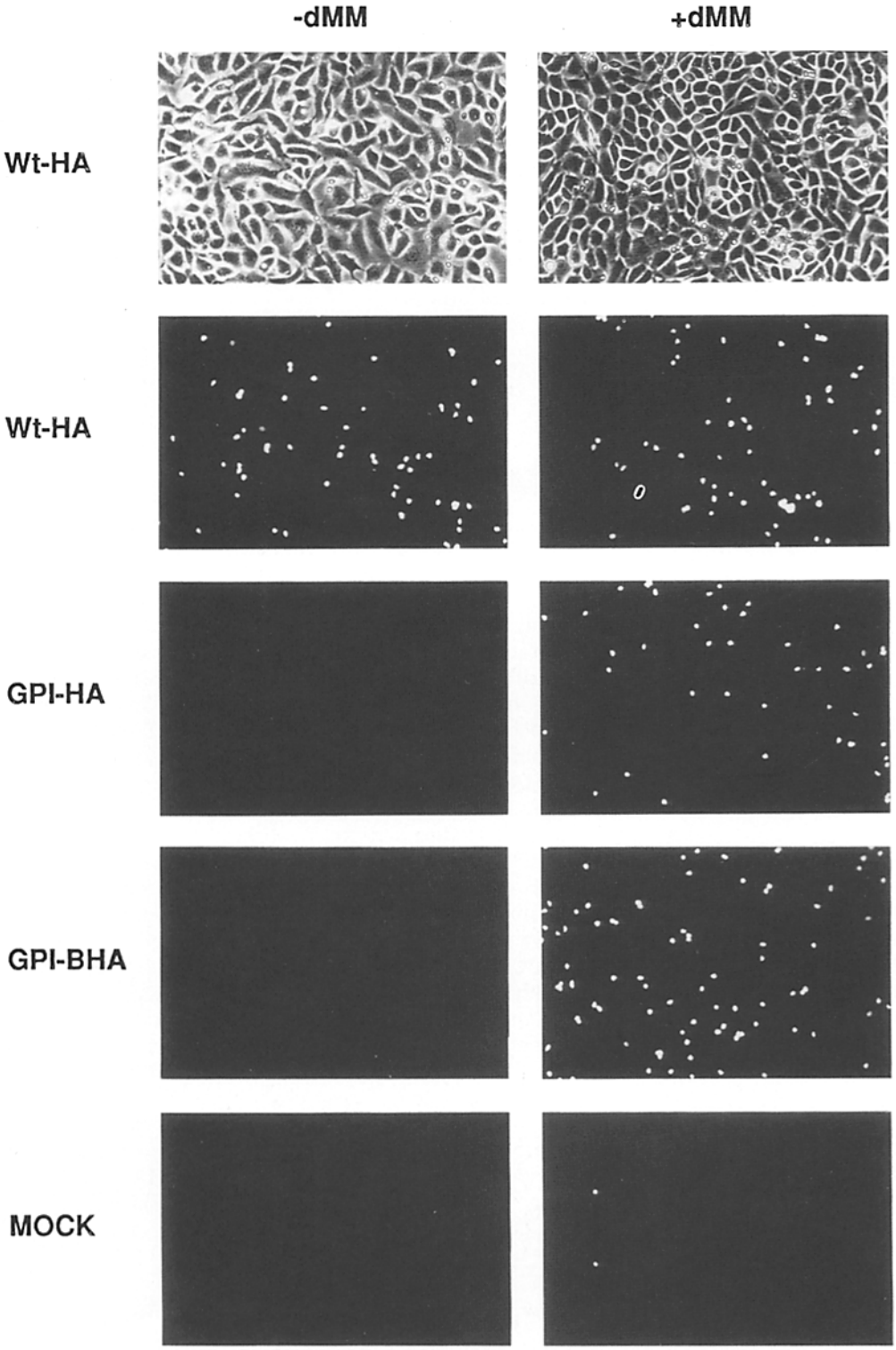

Figure 7. The effect of dMM on the erythrocyte binding activity of wt-HA, GPI-HA, and GPI-BHA. Cells were grown in the presence (*right*) or absence (*left*) of 0.25 mM dMM for 48 h. Confluent monolayers of cells were briefly treated with 0.2 mg/ml neuraminidase and 5 μg/ml trypsin for 5 min at RT before incubation with R_{18} labeled human erythrocytes. Unbound erythrocytes were removed by several washes and the cells photographed with both phase contrast and fluorescence microscopy. The phase contrast is shown for the wt-HA expressing cells only (*top*); all other fields contain an equivalent density of cells. Cells transfected with only the pEE14 vector are in the bottom panels (*MOCK*).

pH forms of both molecules (Table II). Collectively, these results indicate that PI-PLC-released GPI-HA adopts hydrophobic properties after treatment at low pH due to conformational changes that include exposure of the fusion peptides.

Oligomeric Structure of Low pH-Treated GPI-HA

Although wt-HA changes conformational at low pH, it remains trimeric (12). We therefore determined whether GPI-HA remains trimeric after exposure to low pH. Intact cells expressing wt-HA or GPI-HA were biotinylated, exposed to either pH 7.0 or pH 5.2 for 10 min at 37°C, neutralized, and lysed. Lysates were separated on 5–25% sucrose gradients and immunoprecipitated (Fig. 10). The neutral pH forms of membrane-bound wt-HA and GPI-HA cosedimented in the position of 9S trimers (Fig. 10). Although the low pH-treated samples migrated somewhat slower than their neutral pH-

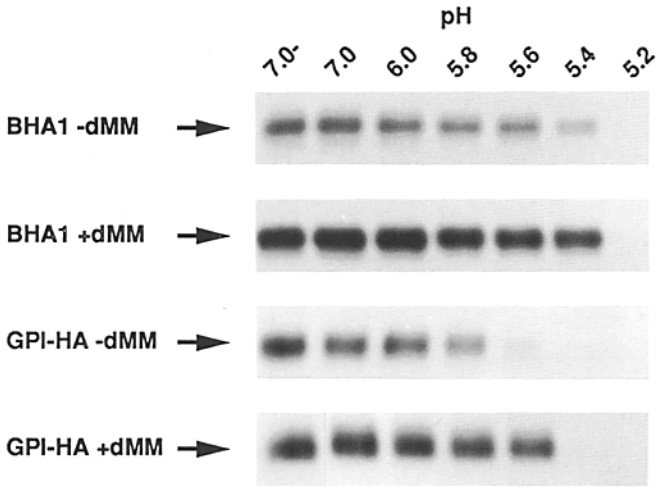

Figure 8. Proteinase K digestion of BHA and PI-PLC-released GPI-HA and the effect of dMM on the pH of the conformational change. Cells expressing either wt-HA or GPI-HA were labeled with [^{35}S]TransLabel for 18 h at 37°C in the absence (*−dMM*) or presence (*+dMM*) of 0.25 mM dMM. BHA and PI-PLC-released GPI-HA were prepared as described in Materials and Methods and aliquots of each sample were treated at the indicated pH by the addition of a predetermined amount of 0.1 M citric acid for 15 min at 37°C. The samples were reneutralized and digested with 0.2 mg/ml PK for 30 min at 37°C. The digestion was stopped by the addition of PMSF and the samples immunoprecipitated with the site A mAb. Immunecomplexes were boiled, reduced, separated on 10% SDS-PAGE, and subjected to fluorography. The pH of each sample is indicated above and the position of the HA1 polypeptide is indicated next to each lane.

Table II. Immunoprecipitation of BHA and PI-PLC-released GPI-HA with pH Specific Antibodies

	BHA			PI-PLC GPI-HA		
Antibody	pH7	pH5	Δ	pH7	pH5	Δ
Fusion peptide	0	109	+109	8	89	+81
N1	87	3	−84	94	4	−90
N2	92	0	−92	87	0	−87

^{35}S-labeled BHA and PI-PLC-released GPI-HA were prepared as described in the legend to Fig. 9. Samples were either maintained at pH7 or treated at pH5, reneutralized, and immunoprecipitated with the indicated antibodies as described in reference 27. Values represent the percent of HA precipitated.

treated counterparts, low pH-treated membrane-bound wt-HA and GPI-HA sedimented similarly (Fig. 10). Chemical cross-linking of the peak fractions from these gradients demonstrated the presence of trimers in all cases (data not shown). This analysis indicated that GPI-HA remains trimeric after exposure to fusion-inducing conditions.

Discussion

Many cellular proteins are tethered to membranes via GPI anchors (3, 10, 18). Transmembrane and GPI forms of the same polypeptide can differ in their rate and route of endocytosis, their destination in polarized cells, or their function (4, 26, 33). For the Qa-2 and Ly-6/E lymphocyte surface molecules, the GPI anchor is essential for signaling function (34, 40). In none of these cases, however, is the role of the GPI anchor understood in terms of the structure of the glycoprotein ectodomain. In this report we assessed the consequences of GPI anchorage on the assembly, posttranslational modifications, lateral mobility, conformational changes, and receptor binding activity of the well-characterized influenza HA. We found that GPI-anchored HA forms stable, laterally mobile trimers that are transported to the cell surface with the same efficiency and rate as wt-HA. Their ectodomains, which can be released as stable trimers with PI-PLC, change conformation, expose their fusion peptides, and become hydrophobic at low pH. Therefore, in many respects the ectodomain of GPI-anchored HA appears identical to that of wt-HA. However, GPI-anchored-HA undergoes additional oligosaccharide processing which completely blocks HA's receptor binding activity. We believe this difference is attributable to the GPI-anchor because chimeras containing the HA ectodomain and the juxtamembrane (both sides) and transmembrane domains of other viral glycoproteins bind to and fuse with target membranes like wt-HA (14, 35).

In wt-HA (X:31 strain) two oligosaccharide chains retain the high mannose form. One is near the "hinge region" and the other is at Asn 165 which lies within 7 Å of the receptor binding site (Fig. 11). Additional oligosaccharide processing, either by growth of virus in MDBK cells (8, 11) or by introducing a new oligosaccharide addition site near the receptor binding pocket (20), inhibits HA's receptor binding activity. We propose that terminal processing of the oligosaccharide chain at Asn 165 of GPI-anchored HA abolishes its erythrocyte binding activity by filling or masking the receptor pocket on a neighboring monomer (Fig. 11).

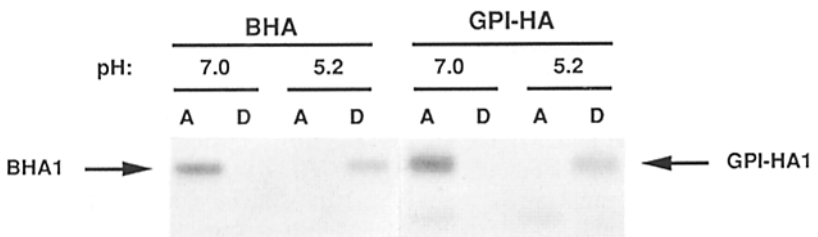

Figure 9. TX-114 partitioning of BHA and PI-PLC-released GPI-HA. Cells expressing wt-HA and GPI-HA were labeled with [^{35}S]TransLabel for 18 h at 37°C in the presence of 0.25 mM dMM. BHA and PI-PLC-released GPI-HA were prepared as described in Materials and Methods. The samples were treated at pH 7.0 or pH 5.2 for 15 min at 37°C, reneutralized and extracted with TX-114. The detergent (*D*) and aqueous (*A*) phases were separated and immunoprecipitated with anti-HA serum. The immunecomplexes were reduced, boiled, and subjected to 10% SDS-PAGE and autoradiography.

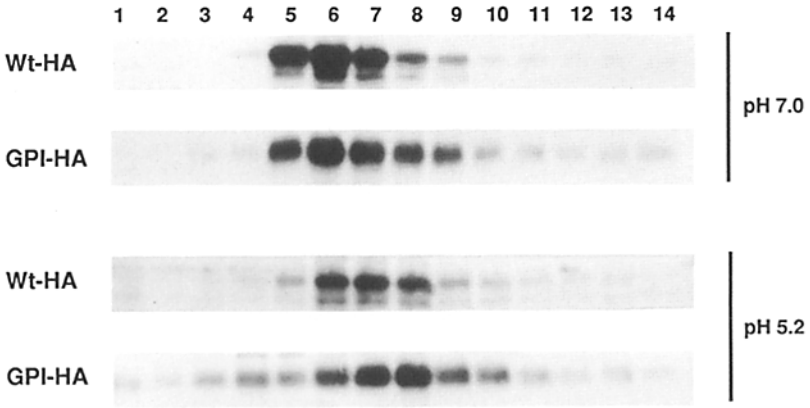

Figure 10. Sucrose gradient analysis of cell surface wt-HA and GPI-HA before and after low pH treatment. Intact cells were briefly trypsinized, biotinylated, and treated at pH 7.0 or pH 5.2 for 10 min at 37°C. The cells were reneutralized and lysed. (*A*) The lysates were sedimented on 5–25% sucrose gradients containing 0.1% NP-40, fractionated, precipitated with the site A mAb, separated on 10% SDS-PAGE and probed with streptavidin-HRP and ECL. The HA1 or GPI-HA1 subunit is shown with the corresponding fraction number listed above each lane. Fractions number 6 of the HA pH7 and GPI-HA pH7 gradients were ~16.5% in sucrose. Fraction number 7 of the HA pH5 and fraction number 8 of the GPI-HA pH 5 gradients were ~15% in sucrose.

The mechanism by which GPI-anchored HA acquires more complex oligosaccharides is not understood. It is unlikely that GPI-anchored HA encounters different intracellular compartments, and hence different glycosidases, because it is transported to the cell surface with similar efficiency and time course as wt-HA. Our favored hypothesis is that the GPI anchor leads to modifications in the structure of the HA ectodomain such that the oligosaccharide chains at Asn 165 and 285, which are normally sequestered, are subjected to terminal glycosylation. This hypothesis is supported by three observations: (*a*) the high mannose oligosaccharide chains attached to Asn 165 and 285 in wt-HA make numerous stabilizing contacts with the polypeptide (50); (*b*) deletion of these oligosaccharide addition sites yields HAs that are less stable or misfolded at 42°C (21); (*c*) the ectodomain of GPI-anchored HA changes conformation at higher pH (0.4 U) than the wt ectodomain (Fig. 8), suggesting that it has fewer stabilizing contacts (reviewed in 49).

The receptor binding defect of GPI-anchored HA could be due to local (near the point of membrane insertion) or long-range (nearer to the membrane distal receptor binding sites) changes in the polypeptide structure. A local change could indirectly affect association of the HA ectodomain with oligosaccharide processing enzymes. Support for this possi-

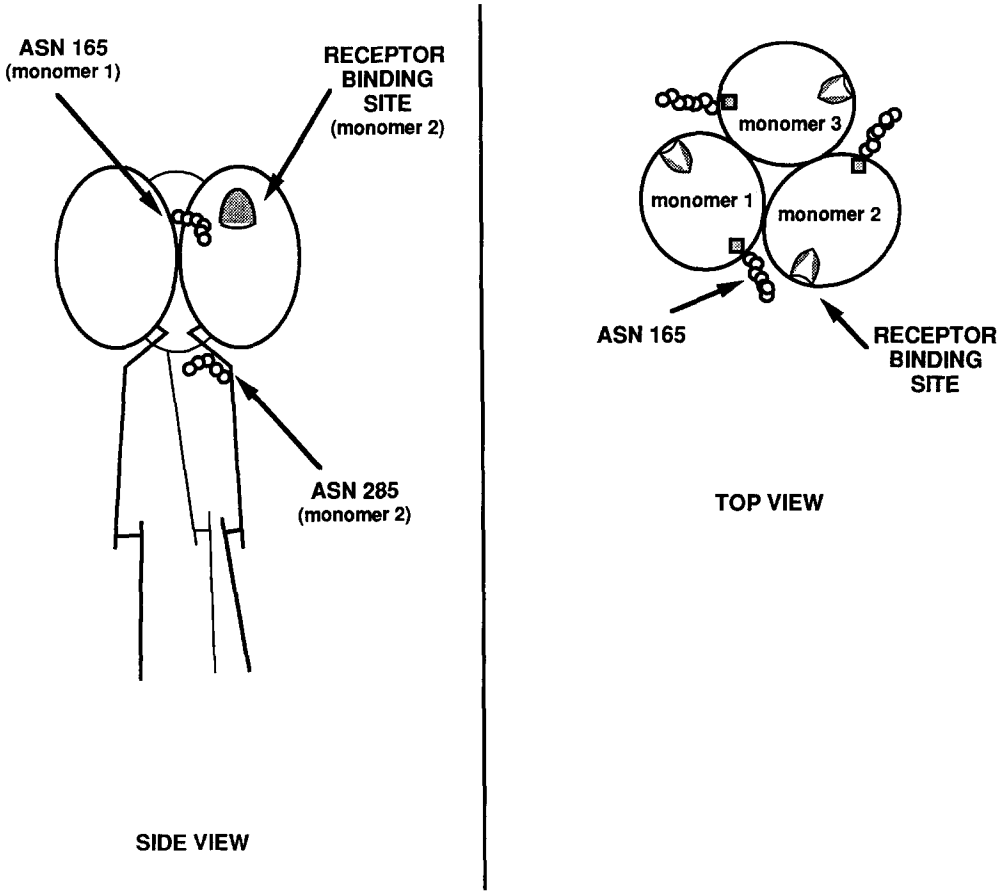

Figure 11. Diagram of the HA trimer indicating the receptor binding site and the oligosaccharide chains at Asn 165 and Asn 285 of HA1. (*Left*) Side view of the HA trimer. (*Right*) Top view of the HA trimer demonstrating the position of the oligosaccharide chain at Asn 165 relative to the sialic acid binding site.

bility comes from the observation of only local structural changes in a pH-shifted HA fusion mutant with an amino acid substitution near the base of the ectodomain (45). Alternatively, the receptor binding defect of GPI-anchored HA could be due to changes in the structure of the protein nearer to the receptor binding sites that directly allow Asn 165 of GPI-anchored HA to receive more complex oligosaccharide chains. Support for this possibility comes from biochemical analyses which suggest that point mutations near the base of the HA ectodomain can affect the packing of the globular head domains and vice versa (23, 27, 51, see Fig. 11). Most importantly, whether the structural differences in the polypeptide are local or long-range, our results show, for the first time, that anchoring a protein to a membrane via a GPI-tail can lead to changes that profoundly affect a functional domain located at a great distance from the point of membrane insertion.

A GPI anchor is essential for the ability of the lymphocyte surface proteins Qa-2 and Ly-6/E to activate T cells (34, 40). To explain this finding, it has been suggested that only the GPI-anchored forms can interact with membrane-associated kinases (3, 38). This could be because transmembrane or cytoplasmic domains prevent association with a kinase, either directly or indirectly. Alternatively, our data suggest that the structures of the GPI-anchored Qa-2 and Ly-6 ectodomains may be uniquely suited to interact with transmembrane kinases or accessory proteins. More generally, the structures of GPI-anchored proteins may differ from their transmembrane-bound counterparts, thus allowing them to interact with specific factors that dictate their unique behaviors. In this manner, GPI anchorage may serve as a powerful means for the cell to alter the structure and function of cell surface proteins.

We thank T. Danieli for the gift of the wt-HA-expressing cell line, O. Gutman for lateral mobility measurements, J. Skehel, I. Wilson, R. Lerner, and A. Helenius for antibodies, A. Bartfay and M. Bhaumik for technical assistance, I. Wilson for a stimulating discussion, S. Green and members of the White lab for critical comments on the manuscript, and H. Czerwonka for manuscript preparation.

The work was supported by a grant from the National Institutes of Health to J. M. White (AI22470).

Received for publication 26 March 1993 and in revised form 24 June 1993.

References

1. Bebbington, C. R., and C. C. G. Hentschel. 1987. The use of vectors based on gene amplification for the expression of cloned genes in mammalian cells. *In* DNA Cloning. D. M. Glover, editor. Academic Press, New York. Vol. 3. 163–188.
2. Boulay, F., R. W. Doms, R. G. Webster, and A. Helenius. 1988. Post-translational oligomerization and cooperative acid activation of mixed influenza hemagglutinin trimers. *J. Cell Biol.* 106:629–639.
3. Brown, D. A. 1992. Interactions between GPI-anchored proteins and membrane lipids. *Trends Cell Biol.* 2:338–343.
4. Brown, D. A., B. Crise, and J. K. Rose. 1989. Mechanism of membrane anchoring affects polarized expression of two proteins in MDCK cells. *Science (Wash. DC).* 245:1499–1501.
5. Burke, B., K. Matlin, E. Bause, G. Legler, N. Peyrieras, and H. Ploegh. 1984. Inhibition of *N*-linked oligosaccharide trimming does not interfere with surface expression of certain integral membrane proteins. *EMBO (Eur. Mol. Biol. Organ.) J.* 3:551–556.
6. Caras, I., G. Weddell, M. Davitz, V. Nussenzweig, and D. W. Martin. 1987. Signal for attachment of a phospholipid membrane anchor in decay accelerating factor. *Science (Wash. DC).* 238:1280–1283.
7. Copeland, C. S., K.-P. Zimmer, K. R. Wagner, G. A. Healey, I. Mellman, and A. Helenius. 1988. Folding, trimerization, and transport are sequential events in the biogenesis of influenza virus hemagglutinin. *Cell.* 53:197–209.
8. Crecelius, D. M., C. M. Deom, and I. T. Schulze. 1984. Biological properties of a hemagglutinin mutant of influenza virus selected by host cells. *Virology.* 139:164–177.
9. Crise, B., A. Ruusala, P. Zagouras, A. Shaw, and J. K. Rose. 1989. Oligomerization of glycolipid-anchored and soluble forms of the vesicular stomatitis virus glycoprotein. *J. Virol.* 63:5328–5333.
10. Cross, G. A. M. 1990. Glycolipid anchoring of plasma membrane proteins. *Annu. Rev. Cell Biol.* 6:1–39.
11. Deom, C. M., and I. T. Schulze. 1985. Oligosaccharide composition of an influenza virus hemagglutinin with host-determined binding properties. *J. Biol. Chem.* 260:14771–14774.
12. Doms, R. W., and A. Helenius. 1986. Quaternary structure of influenza virus hemagglutinin after acid treatment. *J. Virol.* 60:833–839.
13. Doms, R. W., A. Helenius, and J. White. 1985. Membrane fusion activity of the influenza virus hemagglutinin. *J. Biol. Chem.* 260:2973–2981.
14. Dong, J., M. G. Roth, and E. Hunter. 1992. A chimeric avian retrovirus containing the influenza virus hemagglutinin gene has an expanded host range. *J. Virol.* 66:7374–7382.
15. Dotti, C. G., and K. Simons. 1990. Polarized sorting of viral glycoproteins to the axon and dendrites of hippocampal neurons in culture. *Cell.* 62:63–72.
16. Duval, N., E. Krejci, J. Grassi, F. Coussen, J. Massoulie, and S. Bon. 1992. Molecular architecture of acetylcholinesterase collagen-tailed forms; construction of a glycoplipid-tailed tetramer. *EMBO (Eur. Mol. Biol. Organ.) J.* 11:3255–3261.
17. Edidin, M. 1992. Patches, posts and fences: proteins and plasma membrane domains. *Trends Cell Biol.* 2:376–380.
18. Ferguson, M. A. J., and A. F. Williams. 1988. Cell-surface anchoring of proteins via glycosyl-phosphatidylinositol structures. *Annu. Rev. Biochem.* 57:285–320.
19. Fire, E., D. E. Zwart, M. G. Roth, and Y. I. Henis. 1991. Evidence from lateral mobility studies for dynamic interactions of a mutant influenza hemagglutinin with coated pits. *J. Cell Biol.* 115:1585–1594.
20. Gallagher, P., J. Henneberry, I. Wilson, J. Sambrook, and M.-J. Gething. 1988. Addition of carbohydrate side chains at novel sites on influenza virus hemagglutinin can modulate the folding, transport, and activity of the molecule. *J. Cell Biol.* 107:2059–2073.
21. Gallagher, P. J., J. M. Henneberry, J. F. Sambrook, and M.-J. Gething. 1992. Glycosylation requirements for intracellular transport and function of the hemagglutinin of influenza virus. *J. Virol.* 66:7136–7145.
22. Gething, M. J., K. McCammon, and J. Sambrook. 1986. Expression of wild-type and mutant forms of influenza hemagglutinin: the role of folding in intracellular transport. *Cell.* 46:939–950.
23. Godley, L., J. Pfeifer, D. Steinhauer, B. Ely, G. Shaw, R. Kaufmann, E. Suchanek, C. Pabo, J. J. Skehel, D. C. Wiley, and S. Wharton. 1992. Introduction of intersubunit disulfide bonds in the membrane-distal region of the influenza hemagglutinin abolishes membrane fusion activity. *Cell.* 68:635–645.
24. Harlow, E., and D. Lane. 1988. Immunoaffinity purification. *In* Antibodies: A Laboratory Manual. Cold Spring Harbor Laboratory Press, Cold Spring Harbor, New York. 522–523.
25. Jasin, M., K. A. Page, and D. R. Littman. 1991. Glycosylphosphatidylinositol-anchored CD4/Thy-1 chimeric molecules serve as human immunodeficiency virus receptors in human, but not mouse, cells and are modulated by gangliosides. *J. Virol.* 65:440–444.
26. Keller, G., M. W. Siegel, and I. W. Caras. 1992. Endocytosis of glycophospholipid-anchored and transmembrane forms of CD4 by different endocytic pathways. *EMBO (Eur. Mol. Biol. Organ.) J.* 11:863–874.
27. Kemble, G. W., D. L. Bodian, J. Rosé, I. A. Wilson, and J. M. White. 1992. Intermonomer disulfide bonds impair the fusion activity of influenza virus hemagglutinin. *J. Virol.* 66:4940–4950.
28. Kost, T. A., J. A. Kessler, I. R. Patel, J. G. Gray, L. K. Overton, and S. G. Carter. 1991. Human immunodeficiency virus infection and syncytium formation in Hela cells expressing glycosylphosphatidyl inositol-anchored CD4. *J. Virol.* 65:5276–5283.
29. Kunkel, T. A., J. D. Roberts, and R. A. Zakour. 1987. Rapid and efficient site-specific mutagenesis without phenotypic selection. *In* Methods in enzymology: Vol. 154. R. Wu, editor. Academic Press, Inc., NY. 154: 367–382.
30. Lazarovits, J., S. Shia, N. Ktiskakis, M. Lee, C. Bird, and M. Roth. 1990. The effects of foreign transmembrane domains on the biosynthesis of the influenza virus hemagglutinin. *J. Biol. Chem.* 265:4760–4767.
31. Lin, A., B. Devaux, A. Green, C. Sagerstrom, J. Elliott, and M. Davis. 1990. Expression of T cell antigen receptor heterodimers in a lipid-linked form. *Science (Wash. DC).* 249:677–679.
32. Moran, P., H. Raab, W. J. Kohr, and I. W. Caras. 1991. Glycophospholipid membrane anchor attachment. *J. Biol. Chem.* 266:1250–1257.
33. Powell, S. K., B. A. Cunningham, G. M. Edelman, and E. Rodriquez-Boulan. 1991. Targeting of transmembrane and GPI-anchored forms of N-CAM to opposite domains of a polarized epithelial cell. *Nature (Lond.).* 353:76–77.
34. Robinson, P. J., M. Millrain, J. Antoniou, E. Simpson, and A. L. Mellor. 1989. A glycophospholipid anchor is required for Qa-2-mediated T cell activation. *Nature (Lond.).* 342:85–87.
35. Roth, M., C. Doyle, J. Sambrook, and M. Gething. 1986. Heterologous

transmembrane and cytoplasmic domains direct functional chimeric influenza virus hemagglutinins into the endocytic pathway. *J. Cell Biol.* 102:1271–1283.
36. Rothberg, K. G., Y. Ying, J. F. Kolhouse, B. A. Kamen, and R. G. W. Anderson. 1990. The glycophospholipid-linked folate receptor internalizes folate without entering the clathrin-coated pit endocytic pathway. *J. Cell Biol.* 110:637–649.
37. Singh, I., R. W. Doms, K. R. Wagner, and A. Helenius. 1990. Intracellular transport of soluble and membrane-bound glycoproteins: Folding, assembly and secretion of anchor-free influenza hemagglutinin. *EMBO (Eur. Mol. Biol. Organ.) J.* 9:631–639.
38. Stefanova, I., V. Horejsi, I. J. Ansotegui, W. Knapp, and H. Stockinger. 1991. GPI-anchored cell-surface molecules complexed to protein tyrosine kinases. *Science (Wash. DC).* 254:1016–1019.
39. Stegmann, T., R. W. Doms, and A. Helenius. 1989. Protein-mediated membrane fusion. *Annu. Rev. Biophys. Biophys. Chem.* 18:187–211.
40. Su, B., G. L. Waneck, R. A. Flavell, and A. L. M. Bothwell. 1991. The glycosyl phosphatidylinositol anchor is critical for Ly-6A/E-mediated T cell activation. *J. Cell Biol.* 112:377–384.
41. Vestal, D. J., and B. Ranscht. 1992. Glycosyl phosphatidylinositol-anchored T-cadherin mediates calcium-dependent, homophilic cell adhesion. *J. Cell Biol.* 119:451–461.
42. Walter, E. I., W. L. Roberts, T. L. Rosenberry, W. D. Ratnoff, and W. D. Medof. 1990. Structural basis for variations in the sensitivity of human decay accelerating factor to phosphatidylinositol-specific phospholipase C cleavage. *J. Immunol.* 144:1030–1036.
43. Ward, C. W., and T. A. Dopheide. 1981. Amino acid sequence and oligosaccharide distribution of the haemagglutinin from an early Hong Kong influenza virus variant A/Aichi/2/68 (X-31). *Biochem. J.* 193: 953–962.
44. Weis, W., J. H. Brown, S. Cusack, J. C. Paulson, J. J. Skehel, and D. C. Wiley. 1988. Structure of the influenza virus hemagglutinin complexes with its receptor, sialic acid. *Nature (Wash. DC).* 333:426–431.
45. Weis, W. I., S. C. Cusack, J. H. Brown, R. W. Daniels, J. J. Skehel, and D. C. Wiley. 1990. The structure of a membrane fusion mutant of the influenza virus haemagglutinin. *EMBO (Eur. Mol. Biol. Organ.) J.* 9:17–24.
46. Wettstein, D., J. Boniface, P. Reay, H. Schild, and M. Davis. 1991. Expression of a class II major histocompatibility complex (MHC) heterodimer in a lipid-linked from with enhanced peptide/soluble MHC complex formation at low pH. *J. Exp. Med.* 174:219–228.
47. White, J. M. 1992. Membrane fusion. *Science (Wash. DC).* 258:917–924.
48. White, J. M., and I. A. Wilson. 1987. Anti-peptide antibodies detect steps in a protein conformational change: Low-pH activation of the influenza virus hemagglutinin. *J. Cell Biol.* 105:2887–2896.
49. Wiley, D. C., and J. J. Skehel. 1987. The structure and function of the hemagglutinin membrane glycoprotein of influenza virus. *Annu. Rev. Biochem.* 56:365–394.
50. Wilson, I. A., J. J. Skehel, and D. C. Wiley. 1981. Structure of the haemagglutinin membrane glycoprotein of influenza virus at 3 Å resolution. *Nature (Lond.).* 289:366–372.
51. Yewdell, J. W., A. Taylor, A. Yellen, A. Caton, W. Gerhard, and T. Bachi. 1993. Mutations in or near the fusion peptide of the influenza virus hemagglutinin affect an antigenic site in the globular region. *J. Virol.* 67:933–942.
52. Zhang, F., B. Crise, B. Su, Y. Hou, J. K. Rose, A. Bothwell, and K. Jacobsen. 1991. Lateral diffusion of membrane-spanning and glycosylphosphatidylinositol-linked proteins: toward establishing rules governing the lateral mobility of membrane proteins. *J. Cell Biol.* 115:75–84.